

## Interpreting the 3 TeV $WH$ Resonance as a $W'$ boson

Kingman Cheung<sup>1,2,3</sup>, Wai-Yee Keung<sup>4,5,1</sup>, Chih-Ting Lu<sup>2</sup>, Po-Yan Tseng<sup>6</sup>

<sup>1</sup> *Physics Division, National Center for Theoretical Sciences, Hsinchu, Taiwan*

<sup>2</sup> *Department of Physics, National Tsing Hua University, Hsinchu 300, Taiwan*

<sup>3</sup> *Division of Quantum Phases & Devices, School of Physics,*

*Konkuk University, Seoul 143-701, Republic of Korea*

<sup>4</sup> *Department of Physics, University of Illinois at Chicago, IL 60607, USA*

<sup>5</sup> *Department of Physics and Astronomy,*

*Northwestern University, Evanston, IL 60208, USA*

<sup>6</sup> *Kavli IPMU (WPI), UTIAS, The University of Tokyo, Kashiwa, Chiba 277-8583, Japan*

(Dated: October 21, 2021)

### Abstract

Motivated by a local 3.2 – 3.4 sigma resonance in  $WH$  and  $ZH$  in the ATLAS Run 2 data, we attempt to interpret the excess in terms of a  $W'$  boson in a  $SU(2)_1 \times SU(2)_2 \times U(1)_X$  model. We stretch the deviation from the alignment limit of the Equivalence Theorem, so as to maximize  $WH$  production while keeping the  $WZ$  production rate below the experimental limit. We found a viable though small region of parameter space that satisfies all existing constraints on  $W' \rightarrow jj, t\bar{t}, WZ$ , as well as the precision Higgs data. The cross section of  $W' \rightarrow WH$  that we obtain is about 5 – 6 fb.

## I. INTRODUCTION

Recently, the ATLAS Collaboration [1] reported an experimental anomaly in  $WH$  or  $ZH$  production in the  $q\bar{q}b\bar{b}$  final state at  $\sqrt{s} = 13$  TeV with an apparent excess at around 3 TeV resonance mass region. Note that CMS also searched for the same channels [2]. Though they did not claim observing anything peculiar, we can see that there is a visible peak of more than  $2\sigma$  at around 2.7 TeV. Currently, the CMS observation does not support the 3 TeV excess of ATLAS base on the narrow width resonance analysis. The broad width analysis has not been fully studied, and so it is hard to make conclusion for broad width resonance case. We shall focus on interpreting the ATLAS result while we emphasize that the CMS result does not falsify the ATLAS result. The excessive cross section is roughly [1] (which is estimated from the 95% CL upper limits on the cross section curves)

$$\sigma(pp \rightarrow W' \rightarrow WH) \times B(H \rightarrow b\bar{b}) \approx 5 \pm 1.5 \text{ fb} . \quad (1)$$

A similar excess was seen in  $ZH$  production. The local excesses are at about  $3.2 - 3.4\sigma$  for both  $WH$  and  $ZH$  channels at around 3 TeV, while the global significance is about  $2.2\sigma$ . Nevertheless, the boosted hadronic decays of  $W$  and  $Z$  have substantial overlap at about 60% level, which means that it is difficult to differentiate between the  $W$  and  $Z$  bosons. In the following, we focus on the excess interpreted as a 3 TeV  $WH$  resonance.

We attempt to interpret that there is a 3 TeV spin-1 resonance  $W'$  that decays into  $WH$ . The  $W'$  can arise from a number of extended symmetric models, e.g.,  $SU(2)_1 \times SU(2)_2 \times U(1)_X$  [3, 4]. With an additional  $SU(2)$  symmetry, which is broken at the multi-TeV scale, there will be extra  $W'$  and  $Z'$  bosons, whose masses may be similar or differ depending on the symmetry-breaking pattern. Then the decay  $W' \rightarrow WH$  can explain the excess with a resonance structure. Similarly, the  $Z' \rightarrow ZH$  can explain the excess in  $ZH$  production. Here we focus on the  $WH$  channel.

The  $W'$  boson couples to the right-handed fermions with a strength  $g_R$ , independent of the left-handed weak coupling. The  $W'$  boson can then be produced via  $q\bar{q}'$  annihilation. The  $W'$  boson can mix with the standard model (SM)  $W$  boson via a mixing angle, say  $\sin \phi_w$ , so that the  $W'$  boson can decay into  $WZ$  and  $WH$  with a mixing-angle suppression, and right-handed fermions. Previously, there was the 2 TeV  $WZ$  and  $WW$  anomaly which motivated a lot of phenomenological activities. One of the constraints was the  $WH$  constraint because the Equivalence theorem (ET) states that  $\Gamma(W' \rightarrow WZ) \approx \Gamma(W' \rightarrow WH)$  in the heavy

$W'$  limit [5]. In the model that we are considering, it is indeed true in the alignment limit  $\beta \rightarrow \pi/2 + \alpha$ . Here we attempt to explore how much we can deviate from the alignment limit so that the  $WH$  channel can be enhanced while suppressing the  $WZ$ , thus satisfying the constraint from  $WZ$  [6–10], dijet [11, 12], and precision Higgs data [13].<sup>1</sup>

The organization of this note is as follows. In the next section, we describe the  $SU(2)_1 \times SU(2)_2 \times U(1)_X$  model that we consider in this work. In Sec. III, we demonstrate the deviation from the alignment limit. In Sec. IV, we discuss all the relevant constraints. We present the results in Sec. V, and conclude and comment in Sec. VI.

## II. THE $SU(2)_1 \times SU(2)_2 \times U(1)_X$ MODEL

We follow [3, 4] a renormalizable model based on the  $SU(2)_L \times SU(2)_R \times U(1)_{B-L}$  symmetry. In addition to the SM fermions and gauge bosons, this model also contains new gauge bosons  $W'$ ,  $Z'$ , the right-handed neutrinos  $N_R$ , and also some extra scalars from the extended Higgs sector: a complex  $SU(2)_R$  triplet  $T$  and a complex  $SU(2)_L \times SU(2)_R$  bidoublet  $\Sigma$ . We summarize the particle contents and gauge charges in Table I of this  $SU(2)_L \times SU(2)_R \times U(1)_{B-L}$  Model.

TABLE I. The particle contents and gauge charges of the  $SU(2)_L \times SU(2)_R \times U(1)_{B-L}$  Model [3].

Fields	$SU(2)_L$	$SU(2)_R$	$U(1)_{B-L}$
$(u_L, d_L)$	2	1	+1/3
$(u_R, d_R)$	1	2	+1/3
$(\nu_L, l_L)$	2	1	-1
$(N_R, l_R)$	1	2	-1
$\Sigma$	2	2	0
$T$	1	3	+2

We focus on the extended Higgs sector to study the mass and mixing of new gauge bosons  $W'$ ,  $Z'$ . There are two steps of symmetry breaking from two sets of complex scalar fields, separately. First, the  $SU(2)_R$  triplet scalar  $T = (T^{++}, T^+, T^0)$  breaks  $SU(2)_R \times U(1)_{B-L}$  to

<sup>1</sup> The leptonic constraint on  $W'$  and  $Z'$  are so strong that we opt for the leptophobic nature for the  $W'$  and  $Z'$  bosons.

$U(1)_Y$  by acquiring a large vacuum-expectation value (VEV) at the multi-TeV scale.

$$\langle T \rangle = (0, 0, u_T)^T .$$

The heavy masses of  $W'$  and  $Z'$  are set by  $u_T$ . Second, the  $SU(2)_L \times SU(2)_R$  bidoublet scalar,

$$\Sigma = \begin{pmatrix} \Phi_1^{0*} & \Phi_2^+ \\ -\Phi_1^- & \Phi_2^0 \end{pmatrix} , \quad (2)$$

develops a VEV at the electroweak scale  $v = (v_1^2 + v_2^2)^{\frac{1}{2}} \approx 246$  GeV.

$$\langle \Sigma \rangle = \frac{1}{\sqrt{2}} \begin{pmatrix} v_1 & 0 \\ 0 & e^{i\alpha_\Sigma} v_2 \end{pmatrix} = \frac{v}{\sqrt{2}} \begin{pmatrix} \cos \beta & 0 \\ 0 & e^{i\alpha_\Sigma} \sin \beta \end{pmatrix} , \quad (3)$$

which further breaks  $SU(2)_L \times U(1)_Y$  to  $U(1)_Q$ , where  $Q = T_3^L + T_3^R + \frac{1}{2}(B - L)$ . The phase  $\alpha_\Sigma$  is CP-violating, and we do not include its effects in this work. The ratio  $\tan \beta = v_2/v_1$  of two VEV's follows the same notation as two-Higgs-doublet models (2HDM). This symmetry breaking induces a small mixing between the charged gauge bosons.

Explicitly, the field content of  $\Sigma$  is given by

$$\begin{aligned} \Phi_1^0 &= \frac{1}{\sqrt{2}}[v_1 + (-H \sin \alpha + H' \cos \alpha - iA^0 \sin \beta + iG^0 \cos \beta)] , \\ \Phi_2^0 &= \frac{1}{\sqrt{2}}[v_2 + (H \cos \alpha + H' \sin \alpha + iA^0 \cos \beta + iG^0 \sin \beta)] , \\ \Phi_1^+ &= \cos \beta G^+ - \sin \beta H^+ , \\ \Phi_2^+ &= \sin \beta G^+ + \cos \beta H^+ , \end{aligned} \quad (4)$$

with the  $H$  being the observed 125 GeV Higgs boson,  $H'$  the heavy Higgs boson,  $H^\pm$  the charged Higgs boson,  $A$  the pseudoscalar Higgs boson, and  $G^\pm, G^0$  the Nambu-Goldstone bosons.

We are interested in the energy scale  $u_T$  much larger than the electroweak scale  $v$ . Therefore, the scalar fields from the triplet  $T$  are decoupled from the electroweak scale. At the energy scale lower than  $u_T$ , the scalar sector only consists of the bidoublet  $\Sigma$ , which is the same as the 2HDM with the doublet fields  $H_1^T = (\Phi_1^+, \Phi_1^0)^T$  and  $H_2^T = (\Phi_2^+, \Phi_2^0)^T$  [3].

The electrically-charged states,  $W_L^\pm$  and  $W_R^\pm$ , of the  $SU(2)_L$  and  $SU(2)_R$  symmetries will mix to form physical gauge bosons,  $W^\pm$  and  $W'^\pm$ ,

$$\begin{pmatrix} W^\pm \\ W'^\pm \end{pmatrix} = \begin{pmatrix} \cos \phi_w & \sin \phi_w \\ -\sin \phi_w & \cos \phi_w \end{pmatrix} \begin{pmatrix} W_L^\pm \\ W_R^\pm \end{pmatrix} . \quad (5)$$

The  $W_L^\pm - W_R^\pm$  mixing angle  $\phi_w$  satisfies

$$\sin \phi_w = \frac{g_R}{g_L} \left( \frac{m_W}{m_{W'}} \right)^2 \sin 2\beta, \quad (6)$$

and the  $W$  and  $W'$  masses are given by

$$m_W = \frac{1}{2} g_L v, \quad m_{W'} = g_R u_T, \quad (7)$$

where  $g_L$  and  $g_R$  are the  $SU(2)_L \times SU(2)_R$  gauge couplings. We assume that the mass of the right-handed neutrino is heavier than the  $W'$ , such that the decay  $W' \rightarrow l_R N_R$  is kinematically forbidden.

There are other possible decay modes for the  $W'$  into other Higgs bosons [3] if they are kinematically allowed: e.g.,

$$W'^+ \rightarrow H^+ A, ZH^+, W^+ H', W^+ A, H^+ H, H^+ H'.$$

Such decay widths depend on the mass parameters and are highly model dependent, and so we treat the sum of these decay widths as a restricted variable parameter denoted by  $\Gamma_{W'}^{\text{other}}$ .

### III. DEVIATIONS FROM THE ALIGNMENT LIMIT

In this section, we would derive the  $W'WZ$  and  $W'WH$  couplings in this  $SU(2)_L \times SU(2)_R \times U(1)_{B-L}$  model, using the 2HDM convention, by rewriting the bidoublet  $\Sigma$  in terms of two doublets  $(\Phi_1^+, \Phi_1^0)^T$  and  $(\Phi_2^+, \Phi_2^0)^T$  [3]. The deviation from the ET,  $\Gamma(W' \rightarrow WZ) \neq \Gamma(W' \rightarrow WH)$ , can be realized, if the mixing angles  $\alpha$  and  $\beta$  in 2HDM stays away from the alignment limit. Or vice versus, the ET is restored when  $\beta \rightarrow \alpha + \pi/2$ .

The mass mixing term between  $W$  and  $W'$  comes from the bidoublet and is given by, with the VEV's of the decomposed doublets denoted by  $v_1 = v \cos \beta$  and  $v_2 = v \sin \beta$ ,

$$m_{WW'}^2 = 2 \times \frac{g_R}{\sqrt{2}} \frac{v_1}{\sqrt{2}} \frac{g_L}{\sqrt{2}} \frac{v_2}{\sqrt{2}} = \frac{g_R g_L}{2} v_1 v_2. \quad (8)$$

Note that the factor of 2 in front comes from two ways of matchings. So the induced mixing is described by

$$\begin{pmatrix} W \\ W' \end{pmatrix} = \begin{pmatrix} \cos \phi_w & -\sin \phi_w \\ \sin \phi_w & \cos \phi_w \end{pmatrix} \begin{pmatrix} W_L \\ W_R \end{pmatrix}, \quad \sin \phi_w \approx m_{WW'}^2 / m_{W'}^2. \quad (9)$$

Similarly, there is mixing between  $Z$  and  $Z'$ . The mixing angle  $\phi_w$  induces the coupling  $W^\dagger W' Z$  from the gauge vertices  $W_L^\dagger W_L Z$  and  $W_R^\dagger W_R Z$  of different strengths, according to the SM pattern  $T_3^L - Q \sin^2 \theta_W$ . The two contributions sum up to

$$\frac{g_L}{\cos \theta_W} \sin \phi_w \left[ -(0 - \sin^2 \theta_W) + (1 - \sin^2 \theta_W) \right] = \frac{g_L}{\cos \theta_W} \sin \phi_w .$$

$$(\text{coupling of } W'^\dagger W Z) \equiv g_{W'WZ} = \frac{1}{2} \frac{g_L^2 g_R v^2}{m_{W'}^2 \cos \theta_W} \sin \beta \cos \beta = g_R \frac{m_W m_Z}{m_{W'}^2} \sin 2\beta . \quad (10)$$

However, the leading vertex  $W'^\dagger W H$  is given *not* explicitly from the mixing, but derived by the following steps,

$$(\text{coupling of } W'^\dagger W H) \equiv g_{W'WH} = \frac{\partial m_{WW'}^2}{\partial(v_1/\sqrt{2})} \frac{\partial \Phi_1^0}{\partial H} + \frac{\partial m_{WW'}^2}{\partial(v_2/\sqrt{2})} \frac{\partial \Phi_2^0}{\partial H} . \quad (11)$$

Therefore,

$$g_{W'WH} = \frac{g_L g_R v}{2} \left[ -\frac{v_2}{v} \sin \alpha + \frac{v_1}{v} \cos \alpha \right] = g_R m_W \cos(\alpha + \beta) . \quad (12)$$

Similarly, the Goldstone boson  $G^0$ , associated with  $Z$ , also accompanies with  $H$ .

$$(\text{coupling of } W'^\dagger W G^0) \equiv g_{W'WG^0} = \frac{\partial m_{WW'}^2}{\partial(v_1/\sqrt{2})} \frac{\partial \Phi_1^0}{\partial G^0} + \frac{\partial m_{WW'}^2}{\partial v_2/\sqrt{2}} \frac{\partial \Phi_2^0}{\partial G^0} . \quad (13)$$

$$g_{W'WG^0} = \frac{g_L g_R v}{2} i \left[ \frac{v_2}{v} \cos \beta + \frac{v_1}{v} \sin \beta \right] = i \frac{g_L g_R v}{2} [2 \sin \beta \cos \beta] = i g_R m_W \sin 2\beta . \quad (14)$$

In summary,  $g_{W'WG^0} = i g_R m_W \sin 2\beta$ , and  $g_{W'WH} = g_R m_W \cos(\alpha + \beta)$ . Thus, we obtained the decay widths for  $W' \rightarrow WZ$  and  $W' \rightarrow WH$  in the limit  $m_{W'} \gg m_{W,Z,H}$ .

$$\begin{aligned} \Gamma(W' \rightarrow WZ) &\simeq \frac{g_R^2}{192\pi} m_{W'} \sin^2 2\beta , \\ \Gamma(W' \rightarrow WH) &\simeq \frac{g_R^2}{192\pi} m_{W'} \cos^2(\alpha + \beta) . \end{aligned} \quad (15)$$

In the alignment limit,  $\alpha \rightarrow \beta - \frac{\pi}{2}$ , the two widths above become equal. As ET identifies  $G^0$  with the longitudinal  $Z$ , we expect the relations,

$$\Gamma(W' \rightarrow WZ) \approx \Gamma(W' \rightarrow WG^0) \approx \Gamma(W' \rightarrow WH) \text{ as } \alpha \rightarrow \beta - \frac{\pi}{2} . \quad (16)$$

We are going to illustrate the operation of the ET. The longitudinal  $W^+$  is identified with  $G^+ = \cos \beta \Phi_1^+ + \sin \beta \Phi_2^+$  in Eq.(4). The action of  $W'$  moves entries within the same row in the  $2 \times 2$  matrix form of the bidoublet. Therefore the amplitude

$$\mathcal{M}(W' \rightarrow G^+(p^+) G^0(p^0)) = \frac{g_R}{\sqrt{2}} \frac{1}{\sqrt{2}} (\cos \beta \sin \beta + \cos \beta \sin \beta) (p^+ - p^0) \cdot \epsilon' .$$

$$\mathcal{M}(W' \rightarrow G^+(p^+)G^0(p^0)) = \frac{g_R}{2} \sin 2\beta (p^+ - p^0) \cdot \epsilon' . \quad (17)$$

The factor  $(p^+ - p^0)$  corresponds to the Feynman amplitude for the convective current, which is contracted with the polarization vector  $\epsilon'$  of  $W'$ . The above amplitude should give the same width  $\Gamma(W' \rightarrow WG^0)$ . Indeed it is because  $\frac{1}{2}(p^+ - p^0) \cdot \epsilon' = p^+ \cdot \epsilon' \approx m_W \epsilon_L^+ \cdot \epsilon'$ .

On the other hand, we can start from the tri-gauge coupling of the anti-symmetric Lorentz form,

$$\begin{aligned} & (p^+ - p^0) \cdot \epsilon' (\epsilon^+ \cdot \epsilon^0) + (p^0 + P) \cdot \epsilon^+ (\epsilon^0 \cdot \epsilon') + (-P - p^+) \cdot \epsilon^0 (\epsilon' \cdot \epsilon^+) \\ &= (2p^+ \cdot \epsilon') (\epsilon^+ \cdot \epsilon^0) + (2p^0 \cdot \epsilon^+) (\epsilon^0 \cdot \epsilon') - (2p^+ \cdot \epsilon^0) (\epsilon' \cdot \epsilon^+) . \end{aligned}$$

Now using the ET, we concentrate at the longitudinally polarized  $W$  of  $\epsilon^+ \approx p^+/m_W$  and  $Z$  of  $\epsilon^0 \approx p^0/m_Z$ . Up to an over factor  $\frac{1}{m_W m_Z}$ , we obtain

$$\begin{aligned} & (2p^+ \cdot \epsilon') (p^+ \cdot p^0) + (2p^0 \cdot p^+) (p^0 \cdot \epsilon') - (2p^+ \cdot p^0) (\epsilon' \cdot p^+) \\ &= (2p^0 \cdot p^+) (p^0 \cdot \epsilon') = m_{W'}^2 (p^0 \cdot \epsilon') . \end{aligned}$$

Therefore, the longitudinal amplitude from Eq.(10) agrees with the other calculation based on  $G^+G^0$ .

$$\mathcal{M}(W' \rightarrow WZ) = g_R \sin 2\beta p^0 \cdot \epsilon' = \frac{1}{2} g_R \sin 2\beta m_{W'} \hat{\mathbf{p}} \cdot \boldsymbol{\epsilon}' = \frac{1}{2} g_R m_{W'} \cos \theta \sin 2\beta .$$

Integrating out the angular parameter  $\theta$ , the decay width is

$$\Gamma(W' \rightarrow WZ) = \frac{1}{2m_{W'}} \int |\mathcal{M}(W' \rightarrow WZ)|^2 \frac{d \cos \theta}{2} \frac{1}{8\pi} = \frac{g_R^2 \sin^2 2\beta}{192\pi} m_{W'} , \quad (18)$$

which is in agreement with Eq.(15).

Following the similar method, we can verify the coupling of  $WWH$  in this model by using

$$m_{WW}^2 = \frac{g_L^2 v^2}{4} = \frac{g_L^2}{4} (v_1^2 + v_2^2) .$$

Then the coupling of  $WWH$  is

$$g_{WWH} = \frac{\partial m_{WW}^2}{\partial (v_1/\sqrt{2})} \frac{\partial \Phi_1^0}{\partial H} + \frac{\partial m_{WW}^2}{\partial (v_2/\sqrt{2})} \frac{\partial \Phi_2^0}{\partial H} = g_L m_W \sin(\beta - \alpha) . \quad (19)$$

In the alignment limit,  $\beta \rightarrow \alpha + \pi/2$ , the  $WWH$  coupling goes back to the SM Higgs-gauge boson coupling.

Gauge-boson and fermionic couplings of the 125 GeV Higgs boson are now well measured by ATLAS and CMS, especially, the couplings to the massive gauge bosons. The deviations

from the SM values shall be less than about 10%, i.e  $|\sin(\beta - \alpha)| \gtrsim 0.9$ . That implies the allowed range of  $|\cos(\beta - \alpha)| \lesssim 0.44$ . Weaker limits for the couplings to up- and down-type quarks from Higgs precession data also dictate the  $\alpha$  and  $\beta$ 's parameter region. Therefore, in this model framework, the Higgs precision data would set the boundary on the deviation from the alignment limit, and thus restrict the ratio of  $\Gamma(W' \rightarrow WZ)$  and  $\Gamma(W' \rightarrow WH)$ .

The robust and detailed allowed region of  $\alpha$  and  $\beta$  from Higgs precision data depends on different types of 2HDM's. For the allowed parameter region, we refer to Ref. [13], where Type-I, -II, Lepton-specific, and Flipped 2HDMs have been studied. The universal feature from their results, in the small  $\tan\beta \simeq 0.1$  region, the allowed  $\cos(\beta - \alpha)$  is close to the alignment limit, i.e  $|\cos(\beta - \alpha)| \lesssim 0.05$ . This is because the universal up-type quark Yukawa coupling among the 2HDMs is enhanced by factor  $1/\sin\beta$ . For  $\tan\beta \gtrsim 2$  region, only the Type-I case allows more dramatic deviation from the alignment limit. For instance, taking  $\tan\beta = 2.5$ , the allowed range from Higgs precision data is  $-0.37 < \cos(\beta - \alpha) < 0.42$ . Because only in Type-I case, all the up-, down-quark and leptonic Yukawa couplings deviate from SM values by the same factor  $(\cos\alpha/\sin\beta)$ , such that larger  $\tan\beta$  would not enhance any of these couplings, and they are therefore less constrained by Higgs precision data. We shall use the results of Type-I 2HDM obtained in Ref. [13] to restrict the parameter of our model.

#### IV. CONSTRAINTS FROM EXISTING DATA

Recently, both ATLAS and CMS collaborations have published their  $W'$  searches with different decay channels, including fermionic final states  $l^\pm\nu$  [15], dijet [11, 12],  $tb$  [16], and also bosonic final states  $W^\pm Z$  [6–10] at 13 TeV. Here we list all the constraints from these searches in Table II. Here  $j$  includes all light flavors,  $l$  includes  $(e, \mu)$  and  $\nu$  includes  $(\nu_e, \nu_\mu, \nu_\tau)$ . Finally,  $J$  means large- $R$  jets ( $W$  jet or  $Z$  jet).

As we can see from Table II that the strongest constraint comes from  $W'^{\pm} \rightarrow l^\pm\nu$  searches, but here we choose the leptophobic version of the model such that this constraint will not cause serious effects on our results. On the other hand, the dijet constraints from both the ATLAS and CMS analyses rely on the acceptance ( $A$ ) and the width-to-mass ratio ( $\Gamma/M$ ) effects. Note that the dijet limits quoted in Table II are only for the narrow-width resonance scenario. Here we follow their analyses by using  $A = 0.4(0.6)$  for ATLAS [11] (CMS [12])

TABLE II. Different decay mode searches at 13 TeV of  $W'$  with  $m_{W'} \sim 3$  TeV for both ATLAS and CMS constraints. Here  $j$  includes all light flavors,  $l$  and  $\nu$  include  $(e, \mu)$  and  $(\nu_e, \nu_\mu)$ , separately. Finally,  $J$  means large- $R$  jets ( $W$  jet or  $Z$  jet).

	Process	Upper Bound	Ref.
ATLAS	$pp \rightarrow W'^{\pm} \rightarrow l^{\pm}\nu$	$\leq 0.243$ (fb)	[15]
ATLAS	$pp \rightarrow W'^{\pm} \rightarrow jj'$	$\leq 69.5$ (fb)	[11]
CMS	$pp \rightarrow W'^{\pm} \rightarrow jj'$	$\leq 41.7$ (fb)	[12]
CMS ( $tb \rightarrow l^{\pm}\nu bb$ )	$pp \rightarrow W'^{\pm} \rightarrow tb$	$\leq 84.4$ (fb)	[16]
ATLAS ( $W^{\pm}Z \rightarrow JJ$ )	$pp \rightarrow W'^{\pm} \rightarrow W^{\pm}Z$	$\leq 3.0$ (fb)	[6]
ATLAS ( $W^{\pm}Z \rightarrow l^{\pm}\nu qq'$ )	$pp \rightarrow W'^{\pm} \rightarrow W^{\pm}Z$	$\leq 5.5$ (fb)	[7]
ATLAS ( $W^{\pm}Z \rightarrow qq'l^+l^-$ )	$pp \rightarrow W'^{\pm} \rightarrow W^{\pm}Z$	$\leq 10.4$ (fb)	[8]
ATLAS ( $W^{\pm}Z \rightarrow qq'\nu\nu$ )	$pp \rightarrow W'^{\pm} \rightarrow W^{\pm}Z$	$\leq 3.0$ (fb)	[8]
CMS ( $W^{\pm}Z \rightarrow JJ$ )	$pp \rightarrow W'^{\pm} \rightarrow W^{\pm}Z$	$\leq 3.2$ (fb)	[9]
CMS ( $W^{\pm}Z \rightarrow l^{\pm}\nu qq$ )	$pp \rightarrow W'^{\pm} \rightarrow W^{\pm}Z$	$\leq 7.0$ (fb)	[10]

analyses and the width-to-mass ratio effects are from Table 2 in [11] for ATLAS analysis and Table 4 in for CMS analysis [17] to rescale in our case. <sup>2</sup>

Another set of constraints come from the precision Higgs boson data, including the gauge-Higgs couplings, Yukawa couplings, and the  $H\gamma\gamma$  and  $Hgg$  factors. In 2HDMs, such constraints can be recast in terms of  $\tan\beta$  and  $\cos(\beta-\alpha)$ . The excluded region in the parameter space of Type-I 2HDM is shown explicitly in the upper-left panel in Fig. 1 [13].

## V. RESULTS

In Fig. 1, we show the aforementioned experimental constraints on the parameter space of  $SU(2)_L \times SU(2)_R \times U(1)_{B-L}$  model, and include the non-standard  $W'$  decay width  $\Gamma_{W'}^{\text{other}}$ . The red-dotted points satisfy the requirement on the signal cross section

$$\sigma(pp \rightarrow W') \times B(W' \rightarrow WH) \geq 4.5 \text{ fb}, \quad (20)$$

<sup>2</sup> Since we do not find the width-to-mass ratio effects for  $W'^{\pm} \rightarrow tb$  and  $W'^{\pm} \rightarrow W^{\pm}Z$  for either ATLAS or CMS analysis, we therefore conservatively use the original constraints of their publications with the narrow width approximation analysis.

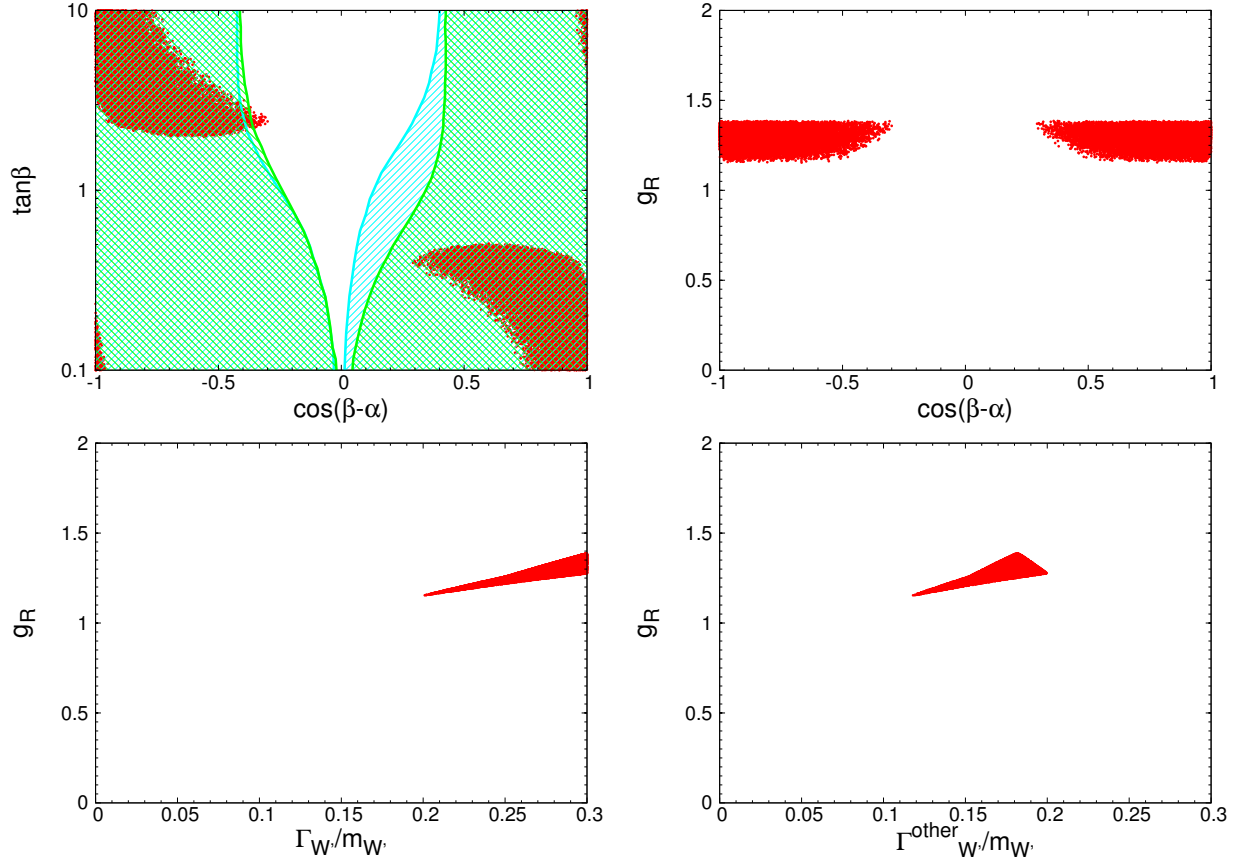


FIG. 1. The red-dotted points for  $m_{W'} = 3$  TeV satisfy the signal production cross section  $\sigma(pp \rightarrow W' \rightarrow WH) \geq 4.5$  fb, the upper limits listed in Table II, and the dijet upper limit adapted for the broad-width resonance. The cyan (green) hatched region was excluded by the Higgs precision data of Type-I 2HDM [13, 14].

evaluated in the narrow-width approximation, and the upper limits listed in Table II, except for the dijet upper limit. The dijet limits are adapted to the broad-width-resonance case, following the instructions in Ref. [11, 17]. The excess bump in the  $m_{JJ}$  distribution of the 2-tag  $WH$  channel from ATLAS [1] is not necessarily a narrow resonance, likewise, we do not restrict the width of  $W'$  to be narrow. The cyan (green) hatched region was excluded by the combined 7 and 8 TeV ATLAS and CMS signal strength data (the ATLAS data only) [13, 14]. The shifting of the hatched region is mainly due to the change in the diphoton signal strength from  $\mu_{\gamma\gamma}(ggF) = 1.32 \pm 0.38$  to  $1.10^{+0.23}_{-0.22}$ . Most of the red-dotted points are ruled out by this constraint, yet there exists a small region that satisfies all the existing constraints and Higgs precision data.

Nevertheless, as shown in Fig 1 there exists a small region of parameter space that is

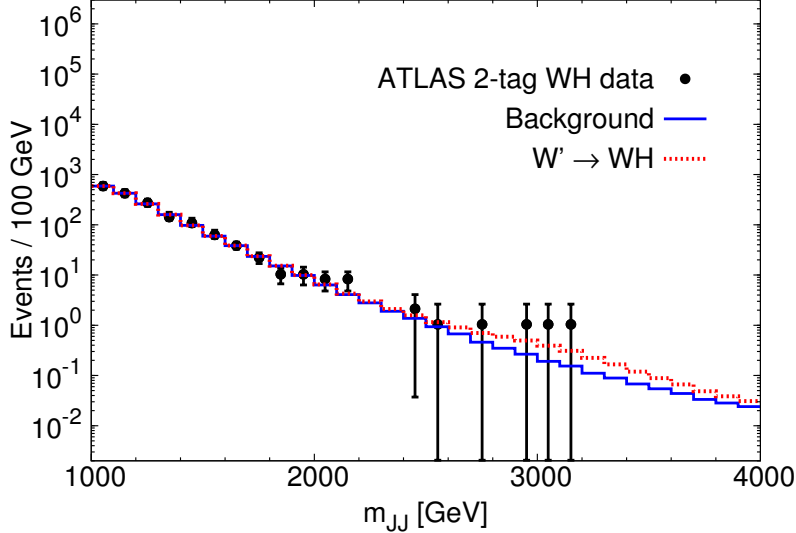


FIG. 2. The  $m_{JJ}$  distribution of ATLAS 2-tag  $WH$  data points and the SM background (blue-solid histogram) are from Ref. [1]. The  $W' \rightarrow WH$  contribution added to the background is indicated with the red-dashed histogram. The parameters are  $\cos(\beta - \alpha) = -0.3$ ,  $\tan\beta = 2.41$ ,  $g_R = 1.358$ ,  $\Gamma_{W'}^{\text{other}} = 0.185 \times m_{W'}$ , and  $m_{W'} = 3$  TeV, which gives  $\sigma(pp \rightarrow W' \rightarrow WH) = 9.7$  fb,  $\Gamma_{W'} = 0.3 \times m_{W'}$ .

not excluded by the aforementioned constraints, including all those listed in Table II (with modified dijet constraints) and the Higgs precision data, as well as satisfying the cross section requirement in Eq. (20). This small region corresponds to parameters  $\cos(\beta - \alpha) \simeq -0.3$ ,  $\tan\beta \simeq 2.41$ ,  $g_R \simeq 1.358$ , and  $\Gamma_{W'}^{\text{other}} \simeq 0.185 \times m_{W'}$ . It will give a cross section of  $\sigma(pp \rightarrow W') \times B(W' \rightarrow WH) \approx 4.6$  fb in the narrow-width approximation. However, if we abandon the narrow-width approximation and adopt the full calculation, it gives a cross section of  $\sigma(pp \rightarrow W' \rightarrow WH) = 9.7$  fb and  $\Gamma_{W'} = 0.3 \times m_{W'}$ . Thus,  $\sigma(pp \rightarrow W' \rightarrow WH) \times B(H \rightarrow b\bar{b}) \approx 5.2$  fb,<sup>3</sup> which is within the range shown by the ATLAS data in Eq. (1). Note that the  $K$  factor for the process is roughly 1.3 at the LHC energies, but for the purpose of consistency with backgrounds we do not multiply this  $K$  factor. Using this point, the  $W'$  contribution to the  $m_{JJ}$  distribution is shown in Fig. 2 with red-dashed histograms, where  $m_{JJ}$  is the invariant mass of the  $W$  and  $H$  hadronic jets. We can see that this broad-width  $W'$  provides an interpretation for the three observed events around  $m_{JJ} = 3$  TeV of ATLAS. Therefore, the allowed region, though small, can explain the excess bump observed at the

<sup>3</sup> We employed the branching ratio  $B(H \rightarrow b\bar{b}) = 0.54$  in 2HDM type-I for  $\cos(\beta - \alpha) = -0.3$  and  $\tan\beta = 2.41$ .

$WH$  channel.

Additional comments are in order here. From the upper-left panel in Fig. 1, the distribution of the red-dotted points is symmetric under the exchange  $\tan \beta \leftrightarrow 1/\tan \beta$  and  $\cos(\beta - \alpha) \leftrightarrow -\cos(\beta - \alpha)$ . It is because the ratio between  $\Gamma(W' \rightarrow WH)$  and  $\Gamma(W' \rightarrow WZ)$  can be rewritten as

$$\frac{\Gamma(W' \rightarrow WH)}{\Gamma(W' \rightarrow WZ)} = \frac{\cos(\beta + \alpha)}{\sin(2\beta)} = \frac{1}{2} \left[ \frac{1}{\tan \beta} - \tan \beta \right] \times \cos(\beta - \alpha) + \sin(\beta - \alpha). \quad (21)$$

Also, from the lower-right panel we can see that without the non-standard decay of  $W'$ , the  $W'$  of  $SU(2)_L \times SU(2)_R \times U(1)_{B-L}$  model does not have any more viable parameter space to explain the  $WH$  excess observed at ATLAS, mainly due to the dijet constraint.

## VI. CONCLUSIONS

We have studied a unified model based on  $SU(2)_L \times SU(2)_R \times U(1)_{B-L}$ , which was broken at multi-TeV scale to the SM symmetry. We have attempted to use the  $W'$  gauge boson of mass 3 TeV to interpret the excess bump seen at the ATLAS  $WH \rightarrow (q\bar{q}')(b\bar{b})$  data. We have shown that such an interpretation faces very strong constraints from dijet data and  $WZ$  data, as well as the precision Higgs data. Yet, we are able to find a viable parameter space region, though small, that can accommodate all the existing data and provide an explanation for the excess bump at 3 TeV. The largest cross section that we obtain is  $\sigma(pp \rightarrow W' \rightarrow WH) \times B(H \rightarrow b\bar{b}) \simeq 5.2$  fb, which is roughly equal to the experimental result shown in Eq. (1).

A few comments are offered as follows.

1. Below the symmetry breaking scale of  $SU(2)_L \times SU(2)_R \times U(1)_{B-L} \rightarrow SU(2)_L \times U(1)_Y$ , the Higgs field can be recast into two doublet Higgs fields, in a manner similar to the conventional 2HDM. Therefore, the model is also subject to the constraints from the precision Higgs data. The ATLAS publication [13] has presented the excluded region in various 2HDM's. We adopted the least restricted one – Type I – in this work, and showed the excluded region in the upper-left panel Fig. 1. All the other types of 2HDM's are more severely constrained, and have no allowed region when superimposed on our model.

2. The mass spectrum of  $A$ ,  $H^+$ , and  $H'$  will have interesting effects on flavor physics and low energy constraints. First of all,  $B$  physics is sensitive to the charged Higgs mass, e.g.,  $b \rightarrow s\gamma$ ,  $B$ - $\bar{B}$  mixing,  $B \rightarrow \mu^+\mu^-$ . However, in Type I 2HDM all Yukawa couplings are proportional to  $\cos\alpha/\sin\beta$ . Therefore, based on the constraint from Higgs precision data,  $\sin(\beta - \alpha) \approx 1$ , and so that  $\alpha \simeq \beta - \pi/2$ . It implies that  $\cos\alpha/\sin\beta \simeq 1$ . Hence, there is no  $\tan\beta$  enhancement in contrast to the Type II model. Therefore, as long as  $\tan\beta \gtrsim 1$ , the constraint on the charged Higgs mass is rather weak. Another important constraint is the  $\rho$  parameter (or  $\Delta T$ ) being very close to 1 – the custodial limit. It can be fulfilled by taking the mass splitting among  $A$ ,  $H'$ ,  $H^+$  to be small. We therefore set  $m_A \approx m_{H'} \approx m_{H^+}$ .
3. We have adopted the leptophobic condition for the  $W'$  boson, or by assuming the right-handed neutrino is heavier than the mass of  $W'$ .
4. Note that the boson jets for  $W$  and  $Z$  bosons are overlapping at 60%. We do not work out for the  $Z' \rightarrow ZH$  boson in this work, but it can be done similarly. However, leptophobic version is a must for the  $Z'$  to avoid the very strong leptonic limit.
5. The dijet limit of  $pp \rightarrow W' \rightarrow jj$  presented the most stringent constraint to the model. We have to adopt other decay modes in order to dilute the branching ratio into dijets. Possible decay modes are  $W'^+ \rightarrow H^+A$ ,  $ZH^+$ ,  $W^+H'$ ,  $W^+A$ ,  $H^+H$ ,  $H^+H'$ . Searches for these modes serve as further checks on the model.
6. The ATLAS data (and also the CMS data) did not indicate a narrow resonance at 3 TeV. Therefore, we assume one more parameter (somewhat restricted)  $\Gamma_{W'}^{\text{other}}$  to alleviate the constraint from dijet. As shown in Fig. 2, the resonance width is rather wide. Currently, we obtained the total width  $\Gamma_{W'} = 0.3 \times m_{W'}$ .
7. Although there are some direct searches on  $A$  and  $H'$  from the LHC [18], the constraints for Type-I 2HDM are not strong enough. Conservatively, we can focus on heavy Higgs bosons around 500 – 1000 GeV, and the interesting signatures for this mass range can

be categorized according to their final states:

- I.  $pp \rightarrow W'^+ \rightarrow H^+ Z/H \rightarrow t\bar{b}b\bar{b} (\tau^+\tau^-) \rightarrow W^+ + 4b$  or  $W^+ + 2b2\tau$  .
- II.  $pp \rightarrow W'^+ \rightarrow H^+ A/H' \rightarrow t\bar{b}t\bar{t} \rightarrow W^+W^+W^- + 4b$  .
- III.  $pp \rightarrow W'^+ \rightarrow W^+ A/H' \rightarrow W^+t\bar{t} \rightarrow W^+W^+W^- + 2b$  .

In the second one, the  $W^+W^+W^-$  can decay into a pair of same-sign dilepton and a pair of jets plus missing energy. Indeed, it has been searched for at the LHC [19]. Many other possibilities of final states consisting of multi-leptons and jets can also be searched for. All these channels are to be explored if the excess of the 3 TeV  $WH$  resonance is going to be established in the future data.

## ACKNOWLEDGMENTS

This research was supported in parts by the MoST of Taiwan under Grant No. MOST-105-2112-M-007-028-MY3, by the U.S. DOE under Grant No. DE-FG-02-12ER41811 at UIC, and by the World Premier International Research Center Initiative (WPI), MEXT, Japan.

- 
- [1] ATLAS Collaboration, “Search for Heavy Resonances Decaying to a  $W$  or  $Z$  Boson and a Higgs Boson in the  $q\bar{q}^{(\prime)}b\bar{b}$  Final State in pp Collisions at  $\sqrt{s} = 13$  TeV with the ATLAS Detector”, ATLAS-CONF-2017-018 (March 2017).
  - [2] CMS Collaboration, “Search for heavy resonances decaying into a vector boson and a Higgs boson in hadronic final states with 2016 data”, CMS PAS B2G-17-002 (March 2017).
  - [3] B. A. Dobrescu and Z. Liu, JHEP **1510**, 118 (2015), [arXiv:1507.01923 [hep-ph]].
  - [4] Y. Gao, T. Ghosh, K. Sinha and J. H. Yu, Phys. Rev. D **92**, no. 5, 055030 (2015), [arXiv:1506.07511 [hep-ph]]. Q. H. Cao, B. Yan and D. M. Zhang, Phys. Rev. D **92**, no. 9, 095025 (2015), [arXiv:1507.00268 [hep-ph]]. P. S. Bhupal Dev and R. N. Mohapatra, Phys. Rev. Lett. **115**, no. 18, 181803 (2015), [arXiv:1508.02277 [hep-ph]].
  - [5] J. Hisano, N. Nagata and Y. Omura, arXiv:1506.03931 [hep-ph]; K. Cheung, W. Y. Keung, P. Y. Tseng and T. C. Yuan, Phys. Lett. B **751**, 188 (2015).

- [6] The ATLAS collaboration [ATLAS Collaboration], ATLAS-CONF-2016-055.
- [7] The ATLAS collaboration [ATLAS Collaboration], ATLAS-CONF-2016-062.
- [8] The ATLAS collaboration [ATLAS Collaboration], ATLAS-CONF-2016-082.
- [9] CMS Collaboration [CMS Collaboration], CMS-PAS-B2G-16-021.
- [10] CMS Collaboration [CMS Collaboration], CMS-PAS-B2G-16-020.
- [11] M. Aaboud *et al.* [ATLAS Collaboration], arXiv:1703.09127 [hep-ex].  
The ATLAS collaboration [ATLAS Collaboration], ATLAS-CONF-2016-069.
- [12] CMS Collaboration [CMS Collaboration], CMS-PAS-EXO-16-056.  
CMS Collaboration [CMS Collaboration], CMS-PAS-EXO-16-032.
- [13] G. Aad *et al.* [ATLAS Collaboration], JHEP **1511**, 206 (2015), [arXiv:1509.00672 [hep-ex]].
- [14] G. Aad *et al.* [ATLAS and CMS Collaborations], JHEP **1608**, 045 (2016), [arXiv:1606.02266 [hep-ex]].
- [15] The ATLAS collaboration [ATLAS Collaboration], ATLAS-CONF-2017-016.  
The ATLAS collaboration [ATLAS Collaboration], ATLAS-CONF-2016-061.
- [16] CMS Collaboration [CMS Collaboration], CMS-PAS-B2G-16-017.
- [17] V. Khachatryan *et al.* [CMS Collaboration], Phys. Rev. D **91**, no. 5, 052009 (2015)  
doi:10.1103/PhysRevD.91.052009
- [18] The ATLAS collaboration [ATLAS Collaboration], ATLAS-CONF-2016-073.  
The ATLAS collaboration, ATLAS-CONF-2016-015.  
V. Khachatryan *et al.* [CMS Collaboration], Phys. Lett. B **755**, 217 (2016), [arXiv:1510.01181 [hep-ex]].  
V. Khachatryan *et al.* [CMS Collaboration], Phys. Lett. B **758**, 296 (2016), [arXiv:1511.03610 [hep-ex]].  
CMS Collaboration [CMS Collaboration], CMS-PAS-HIG-16-010.
- [19] G. Aad *et al.* [ATLAS Collaboration], JHEP **1510**, 150 (2015), [arXiv:1504.04605 [hep-ex]].  
The ATLAS collaboration [ATLAS Collaboration], ATLAS-CONF-2017-030.